Isotopic Diversity Among Meteorites: Implications for the Protoplanetary Disk

Ed Scott[1], Sasha Krot[1], and Ian Sanders[2]

[1] University of Hawai'i, Honolulu, HI 96822; [2]Trinity College, Dublin. escott@hawaii.edu

Introduction: Whole rock $\Delta^{17}O$ and nucleosynthetic isotopic variations for chromium, titanium, nickel, and molybdenum in meteorites define two isotopically distinct populations (Figs. 1-3): carbonaceous chondrites (CCs) and some achondrites, pallasites, and irons in one and all other chondrites and differentiated meteorites in the other [1-5].

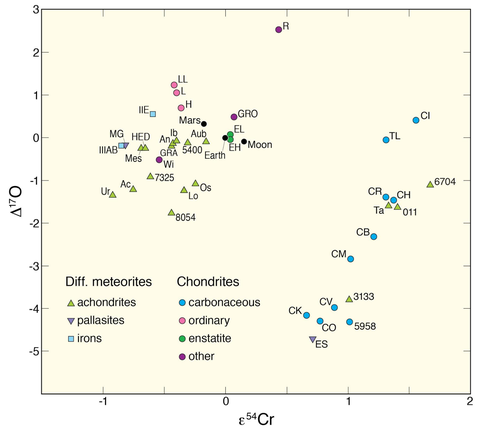

Fig. 1. $\Delta^{17}O$ vs. $\varepsilon^{54}Cr$ for grouped and ungrouped chondrites, differentiated meteorites, and planets showing that they come from two very distinct isotopic reservoirs [1]. Carbonaceous chondrites and a few differentiated meteorites plot on the right; other chondrites, most differentiated meteorites, the Earth, Mars, and the Moon plot on the left side. The gap between the two populations has scarcely decreased since 2011 [1], even though the number of bodies plotted has increased from 27 to 41. Six Cr data points are from Sanborn & Yin et al. 2009-16 abstracts, which contain other data. See [5] for abbreviations and data sources.

Fig. 2. $\varepsilon^{54}Cr$ vs. $\varepsilon^{50}Ti$ for chondrites, differentiated meteorites, and planets, Carbonaceous chondrites and two achondrites, which formed in the outer solar system, are isotopically quite distinct from other chondrites, most differentiated meteorites, and Earth, Mars, and the Moon, which formed in the inner solar system. See [5] for abbreviations and data sources.

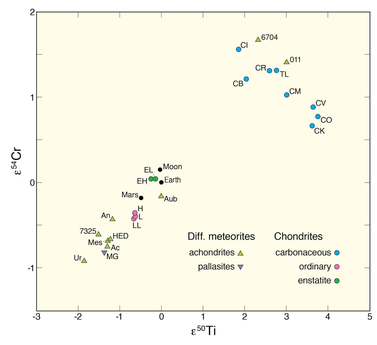

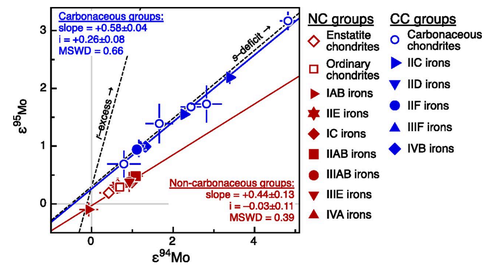

Fig. 3. Kruijer et al. [4] $\varepsilon^{95}Mo$ *vs.* $\varepsilon^{94}Mo$ figure showing that carbonaceous chondrites and related irons (CC: blue points) define a separate line from the data for non-carbonaceous (NC) groups including most irons (red points). Ungrouped irons are mostly CC-related [2, 36].

Implications: Since the isotopic dichotomy persisted in the disk for >3 Myr from the formation of iron meteorite parent bodies [4,18] to the formation of CR chondrules [9, 37], it cannot be attributed to temporal variations in the disk. Instead, the two populations (called CC and NC) were most likely separated in space, plausibly by proto-Jupiter [4]. Here we discuss implications for understanding CAIs, chondrules, planetesimal accretion, and the formation of the asteroid belt.

The Astrophysical Journal, 854:164 (12pp), 2018 February 20 https://doi.org/10.3847/1538-4357/aaa5a5

Ref. [5] Please email reprint requests

Isotopic Dichotomy among Meteorites and Its Bearing on the Protoplanetary Disk

Understanding the distribution of refractory inclusions & elements

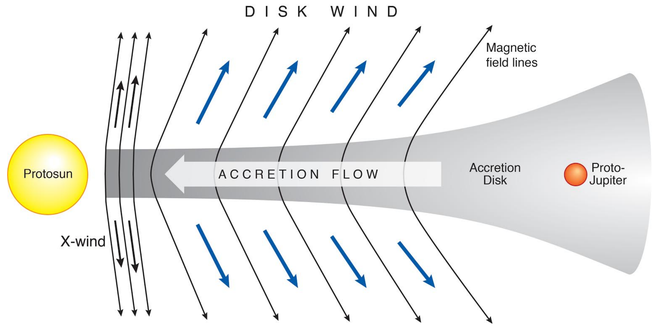

Fig. 4. Cartoon based on [38] showing how refractory inclusions may have been launched by disk winds [46] along magnetic field lines from near the protosun to the disk periphery [5]. Early growth of proto-Jupiter to ~15 $M_\oplus$ could have prevented refractory inclusions from spiraling further into the inner solar system due to gas drag. Once proto-Jupiter reached 10–20 $M_\oplus$, it would have accreted gas creating an inverse pressure gradient causing mm- and cm-sized particles, to pile up. **This can explain how CAIs survived in the disk for several Myr and why carbonaceous chondrites (and comets [7]) are enriched in CAIs, refractories(Fig. 5), and water** [5, 10].

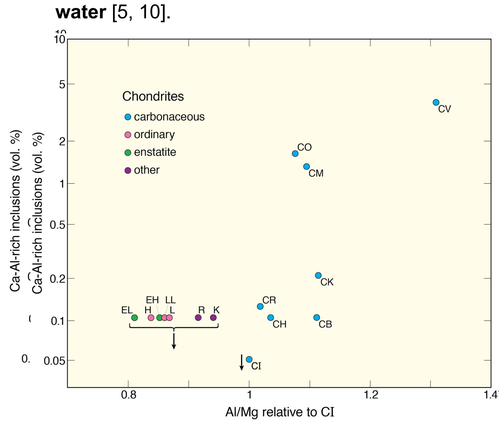

Fig. 5. CAI abundance in chondrites *vs.* Al/Mg ratio normalized to CI chondrites [5]. The enhanced abundance of Al and other refractories in C chondrites probably reflects the addition of CAIs, which are scarce in O, E, and other chondrites. CI chondrites are heavily brecciated and altered and probably once contained more CAIs [47]. Data from [39-40].

Oxygen isotopic compositions of chondrules

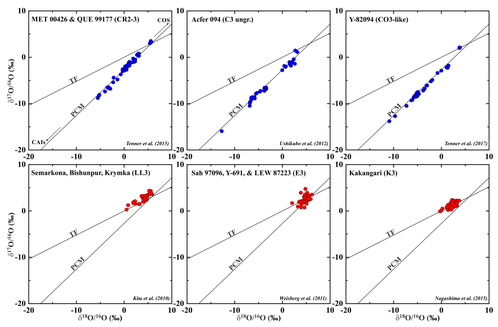

Fig. 6. Plots of $\delta^{17}O/^{16}O$ vs. $\delta^{18}O/^{16}O$ showing olivine and pyroxene compositions in chondrules in carbonaceous (blue) and non-carbonaceous (red) chondrites. Data for CCs spread along the slope-1 primitive chondrule mineral line (PCM) [43], probably due to the abundance of ^{16}O-rich refractory materials and relatively ^{16}O-poor water beyond Jupiter. Data for NCs plot close to the terrestrial mass fractionation line (TF), consistent with the lack of water and refractory material in the inner solar system. Data from [11-14, 42, 43].

Formation of CC and NC reservoirs on either side of proto-Jupiter can help to explain the very different isotopic compositions of chondrules [5, 45]. Other protoplanets may have helped maintain distinct chondrule populations [51] throughout the disk [54].

Accretion time Myr after CAI	≤1 AU	2-3 AU Asteroid belt	> Jupiter	>> Jupiter
4-5				CB chondrites
3-4			CM chondrites	CR chondrites
2-3	E chondrites	H, L, LL R chondrites	CO, CV, CM chondrites	
1-2	IAB irons aubrites		NWA 011, E Sta. pall	
0-1		HEDs, MG pall IC, IIAB, IIIE, IVA	IID, IIF, IIIF, IVB	IIC irons

Time ➔ (vertical) Distance ➔ (horizontal)

Table 1. Inferred accretion times and locations of meteorite parent bodies. Accretion times are inferred from Hf-W and Al-Mg chondrule ages assuming ^{26}Al homogeneity [9, 15, 28], Mn-Cr dating of secondary phases [16], thermal models for ^{26}Al-heated bodies [17, 28, 44], and Hf-W core formation ages [4, 18]. Locations inferred from isotopic constraints [4, 5, 8, 9, 32, 33, 36]. CB chondrites contain outer SS material [8,9], but their formation site is unknown [52, 53].

Implications for chondrule formation

The lack of bodies that accreted in the outer solar system between 1 and 2.5 Myr after CAIs suggests that C chondrites did not accrete until the first generation of planetesimals had melted. **This is consistent with chondrule formation by collision of melted planetesimals, although other planetesimal-induced processes may have operated [19].**

Did partly differentiated asteroids form with chondritic crusts?

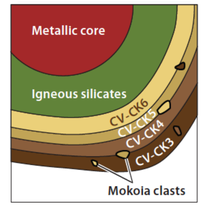

Undifferentiated materials
Chondritic materials, varied metamorphic grade

Differentiated materials
Iron-nickel metal
Igneous silicates (cumulates, bulk magmas, and basaltic extrusions)

Weiss & Elkins-Tanton et al. [20-23] argue that partly differentiated planetesimals like this schematic CV-CK parent body were common as planetesimals may have accreted over 1-2 Myr and preserved their cool, chondritic crusts. Existence of a core dynamo in the CV body was inferred from the magnetization of the Allende matrix [24]. However, this magnetization may instead reflect impact-generated or nebular fields [27, 48, 49]. Continued drag-assisted accretion of chondrules could form chondritic crusts [25] but this is incompatible with the absence of mixtures of genetically-related chondritic and differentiated materials in numerous regolith breccias from the surfaces of the parent bodies of howardites, aubrites, ureilites, and E, R, C, and ordinary chondrites [26]. **Except possibly for the CB chondrites [29], nearly all chondrites and differentiated meteorites are probably derived from separate bodies.**

How did the asteroid belt form?

Three models can account for the origin of CCs and C-type asteroids from beyond Jupiter. Raymond and Izidoro propose that CCs and C-type asteroids are scattered into the asteroid belt as Jupiter grows. In their first model, S-type asteroids formed in the belt [34] but this does not explain why C and S types are roughly equally abundant. In their second model, S types are scattered outwards from ~1 AU [30], but Earth and Mercury formed from E-chondrite-like material, not from OCs and S-type asteroids [32, 33]. In the third, preferred Grand Tack model, Jupiter and Saturn migrated inwards emptying and then repopulating the asteroid belt with roughly equal numbers of planetesimals from inside and outside Jupiter's orbit [35]. **The Grand Tack model accounts for the isotopic dichotomy of meteorites, the mass depletion of the belt, the C/S ratio, and the excited orbits [35]. It should be tested further using isotopic constraints and other meteorite data.**

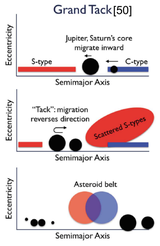

References: [1] Warren P. H. (2011) *GCA* 75, 6912-6926; EPSL 311, 93-100. [2] Budde G. et al. (2016) *EPSL* 454, 293-303. [3] Dauphas N. & Schauble E. A. (2016) *Ann. Rev. Earth. Planet. Sci.* 44, 709-783. [4] Kruijer T. S. et al. (2017) *PNAS* 114, 6712-6716. [5] Scott E. R. D., Krot A. N., & Sanders I. S. (2018) *Astrophys. J.*, 854, 164. [6] Brownlee D. (2014) *Ann. Rev. Earth Planet. Sci.* 42, 179-205. [7] Joswiak D. J. et al. (2017) *MAPS* 52, 1612-1648. [8] Van Kooten E. M. M. E. et al. (2016) *PNAS* 113, 2011-2016. [9] Budde G. et al. (2018) *GCA* 222, 284-304. [10] Morbidelli A. et al. (2016) *Icarus* 267, 368-376. [11] Tenner T. J. et al. (2017) *MAPS* 52, 268-294. [12] Weisberg M. K. et al. (2011) *GCA* 75, 6556-6569. [13] Nagashima K. et al. (2015) *GCA* 151, 49-67. [14] Kita N. T. et al. (2010) *GCA* 74, 6610-6635. [15] Krot A. N. & Nagashima K. (2017) *Geochem. J.* 51, 45-68. [16] Doyle P. M. et al. (2015) *Nature Comm.* 6, 7444 (10 pp). [17] Sugiura N., & Fujiya W. (2014) *MAPS* 49, 772-787. [18] Kruijer T. S. et al. (2014) *Science* 344, 1150-1154. [19] Krot A. N. et al. (2017) *LPI Contrib.* 1963, #2009. [20] Weiss B. P. et al. (2010) *Space Sci. Rev.* 152: 341–390. [21] Weiss B. P. & Elkins-Tanton L. T. (2013) *Ann Rev. Earth Planet. Sci.* 41, 529-560. [22] Elkins-Tanton L. T. et al. (2011) *EPSL* 305, 1-10. [23] Fu R. et al. (2017) in *Planetesimals*, L. T. Elkins-Tanton & B. P. Weiss, eds, 115-135, CUP. [24] Carpozen L. et al. (2011) *PNAS* 108, 6386-6389. [25] Johansen A. et al. (2015) *Sci. Adv.* 1, e1500109. [26] Bischoff A. et al. (2006) In *MESS II*, D. S. Lauretta & H. Y. McSween, eds, 679-712, Arizona. [27] Bland P. et al. (2014) *Nat. Commun.* 5:5451 (13 pp). [28] Nagashima K. et al. (2017) *GCA* 201, 303-319. [29] Oulton J. et al. (2016) *GCA* 177, 254–274. [30] Raymond S. N. & Izidoro A. (2017) *Sci. Adv.* 3: e1701138. [31] Burbine T. H. (2014) in *Treatise on Geochemistry,* 2nd ed., Vol. 1, A. M. Davis, ed., 365-414, Elsevier. [32] Dauphas N. (2016) *Nature* 541, 521-524. [33] McCoy T. J. & Bullock E. S. (2017) in *Planetesimals*, L. T. Elkins-Tanton & B. P. Weiss, eds, 71-91, CUP. [34] Raymond S. N. & Izidoro A. (2017) *Icarus* 297, 134-138. [35] Walsh K. J. et al. (2011) *Nature* 475, 206-209. [36] Worsham E. et al. (2017) *EPSL* 467, 157-166. [37] Schrader D. et al. (2017) *GCA* 201, 275-302. [38] Salmeron R. & Ireland T. R. (2012) *EPSL* 327/8, 61-67. [39] Scott E. R. D. & Krot A. N. (2005) *ASP Conf. Series* 341, 15-53. [40] Hezel D. et al. (2008) *MAPS* 43, 1879-1894. [41] Ebel D. S. et al. (2016) *GCA* 172, 322-356. [42] Tenner T. J. et al. (2015) *GCA* 148, 228-250. [43] Ushikubo T. et al. (2012) *GCA* 90, 242-264. [44] Hunt A. C. et al. (2018) *EPSL* 482, 490-500. [45] Gerber S. et al. (2017) *ApJL* 841, L17. [46] Bjerkeli P. et al. (2016) *Nature* 540, 406-409. [47] Frank D. R. et al. (2017) *MAPS* 52, 6355. [48] Muxworthy A. R. et al. (2017) *MAPS* 52, 2132-2146. [49] Tarduno J. A. Et al. (2016) *LPS* 47, 2609. [50] Morbidelli A. & Raymond S. N. (2016) *JGR Planets* 121, 1962-1980. [51] Jones R. H. (2012) *MAPS* 47, 1176-1190. [52] Bollard J. et al. (2015) *MAPS* 50, 1197-1216. [53] Johnson B. C. et al. (2016) *Sci Adv.* 2, e1601658. [54] Melosh H. J. et al. (2018) LPSC 49, 1673.